Rev. Adv. Mater. Sci. 45 (2016) 8-14

A FACILE DOPING OF GRAPHENE OXIDE NANOSHEETS

A.N. Fouda[1,2], El Shazly M. Duraia[1,3] and Farid El-Tantawy [1,4]

[1]Physics department, Faculty of Science, Suez Canal University, 41522 Ismailia, Egypt
[2]Recruitment department, University of Hail, Hail 2440, KSA
[3]Texas State University-San Marcos, Department of Chemistry and Biochemistry, 601 University Dr., San Marcos, TX 78666, USA
[4]Centre of Nanotechnology, King Abdul Aziz University, Jeddah, Saudi Arabia

Received: October 18, 2015

Abstract. One step and facile synthesis of SnO_2 doped graphene oxide (GO) nanoparticles were conducted by applying a new doping method based on modified Hummer method. The structural and thermal behavior were investigated by X-ray diffraction (XRD), scanning electron microscopy (SEM), transmission electron microscopy (TEM), Raman spectroscopy, and thermal gravitational analysis (TGA). GO sheets exhibited scrolling and crumpling morphology. SnO_2 was embedded in graphite during the initial stage of modified Hummer method and the surface morphology has aggregated lamellar structure with wrinkles. In Raman spectra, the characteristic D-band and G-band were observed in all the samples and the change in their ratio is attributed to the provided defects. The effect of incorporating tin nanoparticles in GO on the electrochemical behavior was investigated. The specific capacitance increases from 113 F/g to 355 F/g after SnO_2 doping. The better electrochemical behavior, the enhancement of conduction and capacitance is mainly related to the insertion of SnO_2 nano particles which act as a well decorated spacers for GO nanosheets and the mechanical strength of GO prevents the volumetric expansion of SnO_2 networks.

1. INTRODUCTION

Recently, an extensive attention was attracted to the fabrication supercapacitors due to the widespread of portable electronic devices, and implantable medical devices. However, to power electric vehicles as well as hybrid vehicles, supercapacitors with higher energy density is required. This can be achieved using electrodes with relatively high capacity. Graphite and other high surface area carbon nanostructures have been widely used in these applications due to its thermal and mechanical stability during charging and discharging process [1-3].

SnO_2 have high theoretical specific capacitance (992 $mAhg^{-1}$), highly reversible reaction mechanism, high Li storage potential, and volumetric energy density is higher than graphite by nine times (7262 $mAhcm^{-3}$) [4,5]. Graphene is a recently investigated mono layer of Sp2 hybridized carbon atoms arranged in a honeycomb structure, has attracted much attention due to its superior properties and wide range of applications [6,7]. Graphene can be used as a host material for SnO_2 nano-particles because of the attached function groups which can act as a nucleation sites [8,9].

However, during electrochemical reaction, the high volumetric strain of SnO_2 (greater than 250%), lead to poor cyclic performance and break down the anodic connection. Some researchers tried to decrease the volumetric change by using SnO_2 in nano-scale or graphene doped SnO_2 nano-composites. Although, graphene exhibited high cycling stability, the reported capacity of graphene as an anode material in LIBs is low (100 $mAhg^{-1}$) [10].

Corresponding author: A.N. Fouda, e-mail: alynabieh@yahoo.com

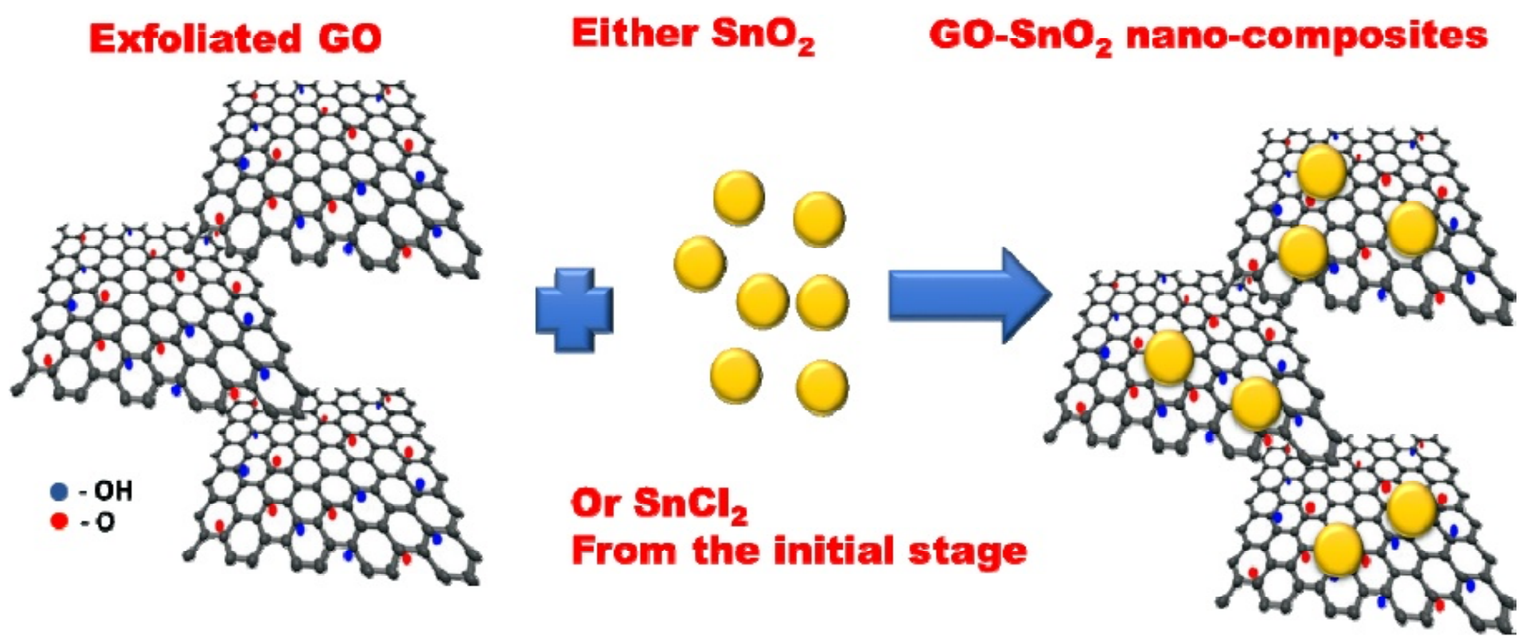

Fig. 1. Schematic diagram describes the doping of GO from the initial stage.

Junfei *et al.* clarified that, getting the advantages of high capacity SnO_2 and promising (excellent) cyclic performance of graphene can lead to high capacity and good cyclic performance composites [11-14]. The synthesis of graphene tin nano composites has been conducted by different methods, such as chemical doping, and hydrothermal method. However, the aggregations of SnO_2 are difficult to avoid [15,16].

In the present work, we report a novel, facile and one step approach to prepare GO-SnO_2 nano-composite based on modified Hummer method. This method is almost identical to the modified Hummer method except enrolling the required dopants at the initial stage. The prepared Nano-composite showed higher capacitance compared to GO. This method is not limited to a distinct doping composite but can be generalized to a wide scale of graphene nano-composites.

2. EXPERIMENTAL

2.1. Preparation of nano-composites

A slight modification was done on the modified Hummer method [17]. One step synthesis of SnO_2 doped GO (S1) and $SnCl_2$ doped GO (S2) was performed. Our approach is based on dissolving SnO_2 and $SnCl_2$ in sulfuric acid at the initial stage which permits a complete solubility and homogenous distribution of SnO_2 through the nan-composites, Fig. 1. Firstly, 0.1 g SnO_2 was dissolved in 23 mL of sulfuric acid. The prepared SnO_2 in sulfuric acid was mixed with 1.0 g of commercial graphite powder and 0.5 g of sodium nitrate within an ice bath, Slowly, we added 3 g of potassium permanganate while stirring for 2 hours. The mixture was kept in water bath at 35 ^oC and stirred for 0.5 hour. The solution temperature was kept at 95 ^oC while adding 46 ml of deionized (DI) water and stirring was continued at the maintained temperature for another 0.5 hour. Then, 10 mL of hydrogen peroxide and 140 mL of deionized (DI) water were added to terminate the reaction. In the case of sample 2 (S2), Similar procedure was repeated after dissolving 0.1 g $SnCl_2$ in 23 mL of sulfuric acid. The color of the mixtures was dark yellow. The product was rinsed with 5% HCl. Filtration Washing were done for several times. Finally, we obtained nan-composite powder after drying at 60 ^oC.

2.2. Characterizations

XRD measurements were performed using Burker D8 diffractometer with Cu K_α radiation. The local vibration modes have been investigated by Raman spectroscopy measurements at room temperature. Micro-Raman spectroscopy system (Model Renishaw system 2000) using Ar+ laser with power of 100 mW and at wavelength of 488 nm has been used. The surface morphology features were investigated using nano-lab Helois 400 attached by EDX. The characterizations were extended to cyclic voltammetry analysis using biologic science instrument VSP with 1 M H_2SO_4 as an aqueous electrolyte at room temperature. The voltage window for CV tests was enclosed between 0.5 and 2 V at scan rates of 30 mV, 50 mV, 70 mV, 100 mV, and 200 mV respectively. Saturated calomel electrode and platinum foil electrode were served as the reference and the counter electrodes, respectively. The glassy carbon (GC) electrodes were polished, subsequently cleaned in organic solvents and rinsed in distilled water. The cleaned GC electrode was coated with GO, S1, and S2 respectively and served as working electrode.

3. RESULTS AND DISCUSSION

Representative XRD patterns of GO, S1, and S2 are shown in Fig. 2. An intensive (001) GO peak can be observed at 10.4^o and the detectable expand

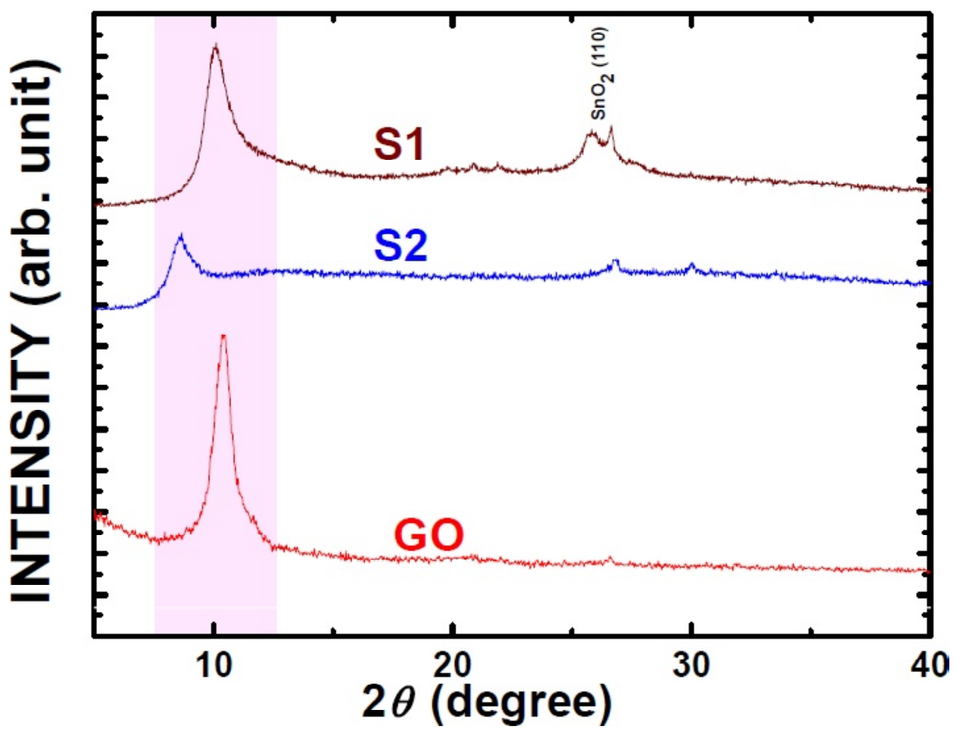

Fig. 2. X-ray diffraction patterns for GO, SnO_2 doped GO (S1), and $SnCl_2$ doped GO (S2).

of the inter-layer spacing to 0.87 is attributed to the introduction of oxygen containing function groups during the exfoliation process which is related to Van deer Waals force between GO layers [18]. Figs. 2c and 2d) shows the characteristic standard (110) peak of SnO_2 beside the existence of the distinguishable GO peak [19].

The morphology of the samples has been investigated using SEM. Scrolling and crumpling morphology can be considered as intrinsic property of GO [19-21]. We reported previously a few layers of perfect hexagonal GO nano-sheets [18, 22]. Fig. 3 shows wide areas of few exfoliated GO expanded layers with long wrinkles and crumpled paper like morphology. As shown in Fig. 4a, S1 exhibited aggregated lamellar structure with wrinkles of GO layers connected to each other. SnO_2 nanoparticles cannot be identified easily because of its well embedding during the initial synthesis stage. The stacking of GO nano sheets is prevented to some extent since SnO_2 Nano particles act as a spacer which prevent the stacking. Fig. 4b shows that the morphology of S2 is similar to S1, revealing that SnO_2 nanoparticles distributed was governed during the initial preparation stage. Furthermore, the composition of nano particles was confirmed by EDX measurements, which revealed the existence of Sn within the composites as tabulated in Table 1.

Raman spectroscopy has been conducted at room temperature in order to study the graphitic quality of the prepared samples. A significant change in the graphitic quality was confirmed using Raman analysis. Fig. 5 displays a comparison of the Raman spectrum of S1, S2, and GO. As one can see from the spectrum there are several peaks. The first two peaks at about 1341 cm^{-1} and 1572 cm^{-1} can be attributed to the D-band and G-band respectively [23]. It is well known that the peak at 1572 cm^{-1} is assigned for the first order phonons scattering (E2g) and the other peak around 1355 cm^{-1} is due to the disorder and defects arise in the sp2 carbon rings (D-band). It is well known that the ratio between the

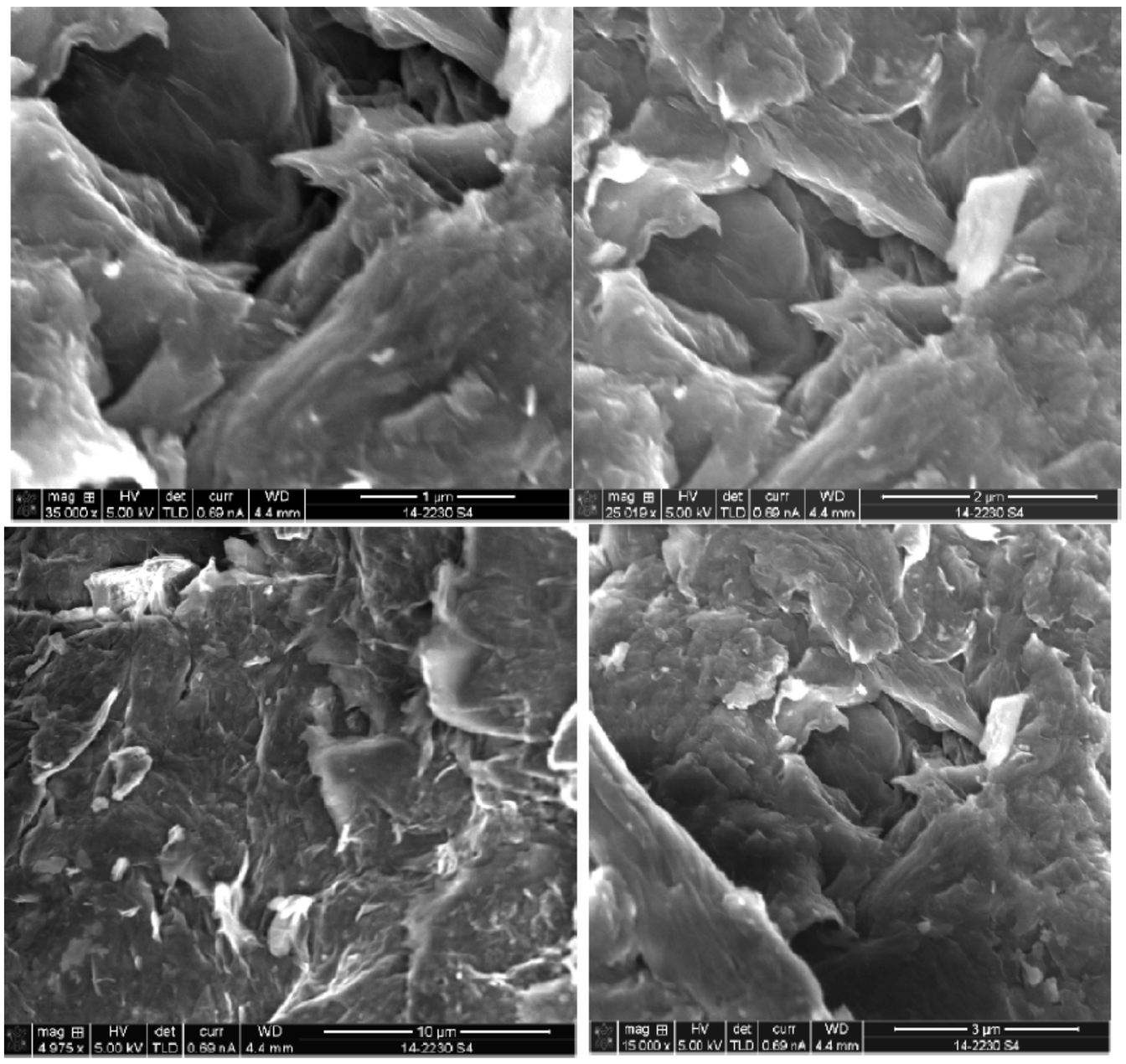

Fig. 3. SEM images of GO nano-sheets with folds and crumbles.

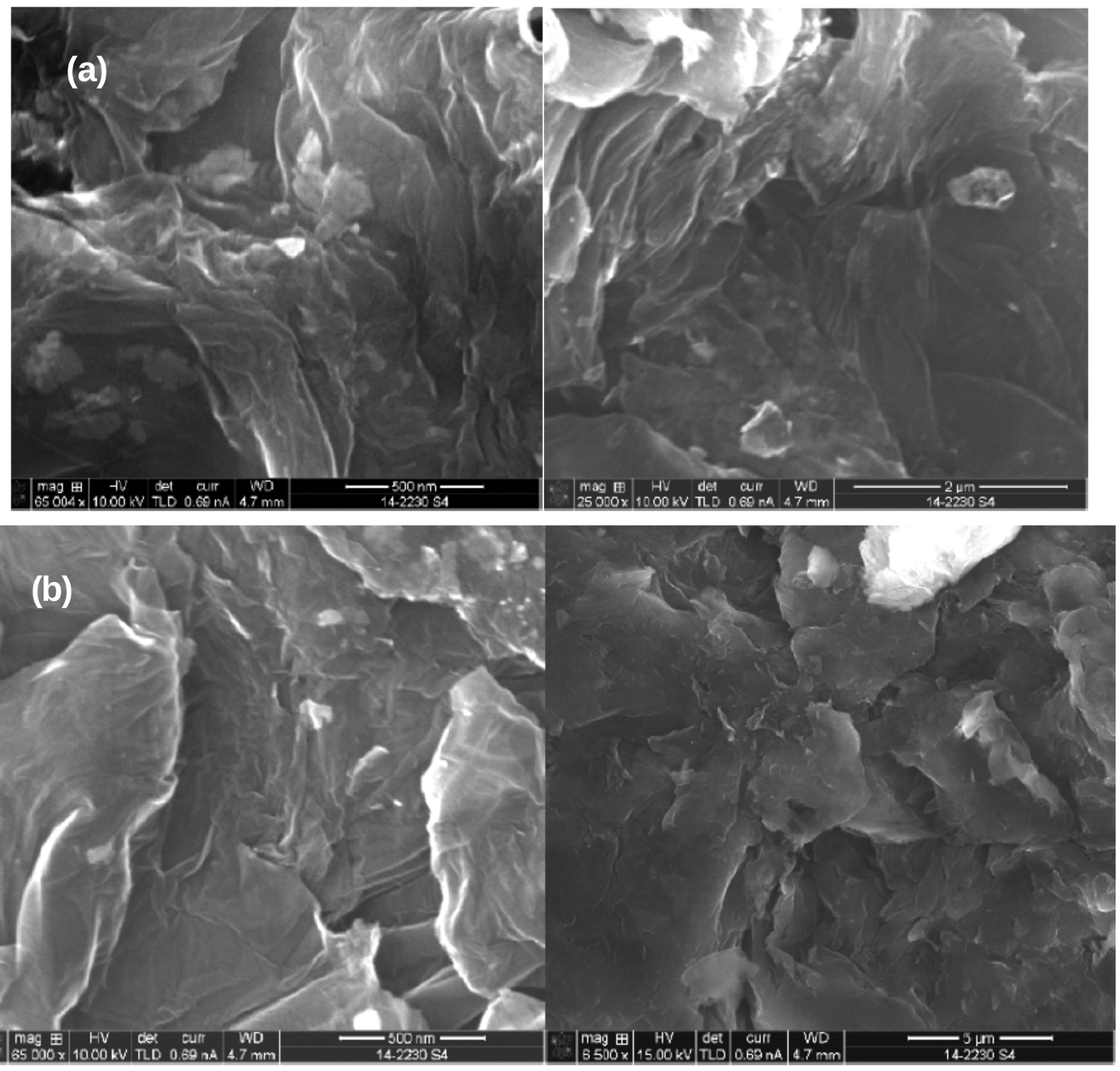

Fig. 4. (a) SEM images of S1 with wrinkles and aggregated lamellar structure and (b) SEM images of S2 with similar morphology to S1.

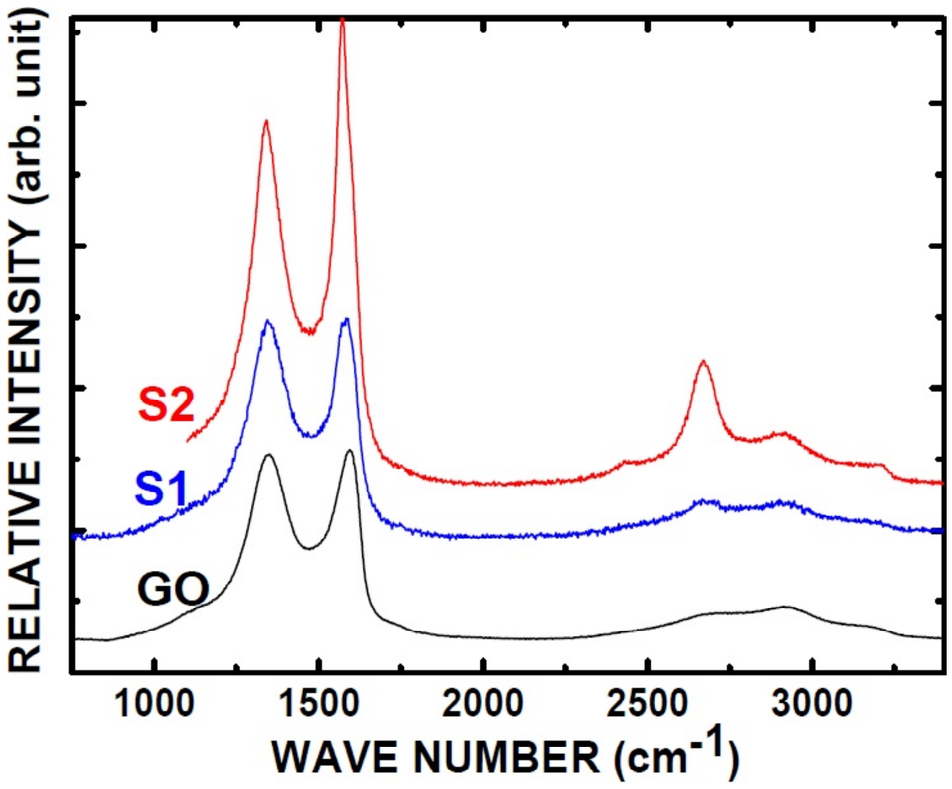

Fig. 5. Raman spectrum of GO, S1, and S2.

intensities of G-band to D-band (I_G/I_D) is corresponding to the quality of the prepared GO [24, 25]. The ratio of I_G/I_D has found to be 1.26. This result indicates that GO has less defects. The relatively sharp peak centered at 2662 cm^{-1} could be attributed to the 2D-band for graphene. The presence of the 2D-band in the Raman spectrum of graphene oxide is very rare and indicates the higher quality of synthesized graphene by the present simple method. The interactions between SnO_2 Nano particles and GO sheets were identified using the change in relative intensity of Raman D and G peak [26]. The corresponding relative intensities of S1 and S2 were 1.01 and 1.21 respectively. Comparing with the relative intensity of GO (0.98), the SnO_2 nanoparticles reduces the number of defects by attaching to the dangling bonds.

The thermal stability of S1 and S2 and the mass percentage of SnO_2 were quantified using TGA measurements as shown in Fig. 6. A drop in weight can be observed around 100 ^oC due to the loss of water. On the other hand, Dehydration and desorption of attached gases from the surface of the synthesized nano-composites takes place around 240 ^oC and 200 ^oC for S1 and S2 respectively. The stability of SnO_2 can be realized and the residual amount of SnO_2 is 43% in both samples [27].

The electrochemical performance of S1 and S2 were investigated through CV measurements by

Table 1. EDX elemental analysis of the synthesized composites.

Elements	GO	S1	S2
C K	79.57	72.78	76.03
O K	20.43	26.56	23.34
Cl K	—	0.25	0.43
Sn L	—	0.41	0.20

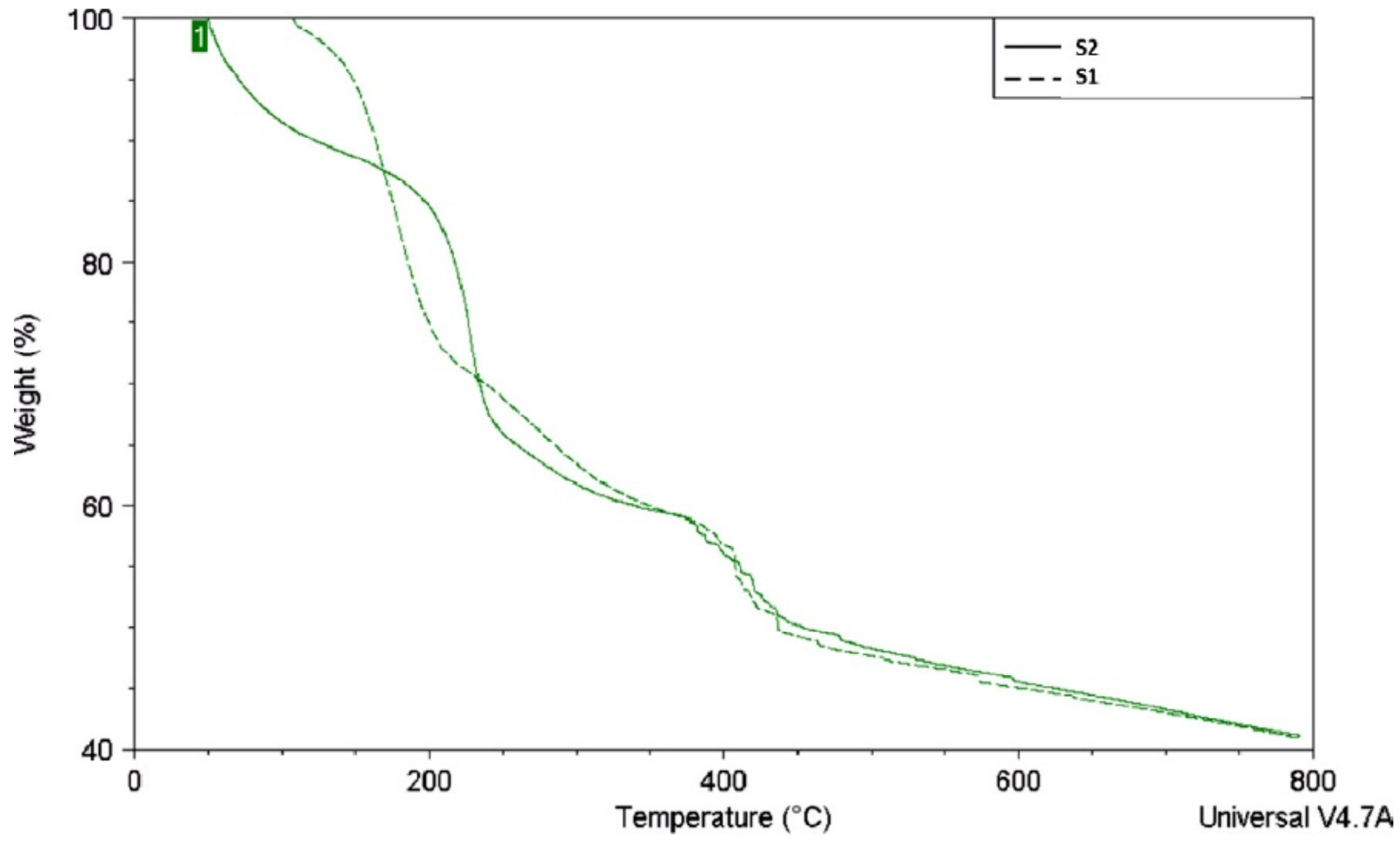

Fig. 6. Thermal gravitational analysis (GTA) of S1 and S2.

using 1.0 M H_2SO_4 as an electrolyte and the electrochemical characteristics of the synthesized GO Nano-sheets can be found elsewhere[18]. CV curves of the samples for different cycle number is show in Figs. 7a and 7b. Almost rectangular CV curves is shown in Figs. 7a and 7b, reflecting the capacitive behavior with two redox peaks, indicating the oxidation and reduction process [28]. For both samples, a little increment in current with increasing the number of cycles is recorded without distortion from the symmetric rectangular shape with redox peaks. A decrease in the discharge curve can be observed with increasing the cycle number and with subsequent charge/discharge, an improvement in the reversibility of the electrode was established [29].

The CV curves for S1 and S2 at different scan rates with a potential window from -0.4~1V, is shown in Figs. 7c and 7d. With increasing the scan rate the redox peak is shifted because of the variation in the electrode resistance. The typical capacitive behavior of increasing the current with increasing the scan rate is established [30]. On the other hand, a detectable distortion from the perfectly rectangular shape was observed with increasing the scan rates, as shown in Figs. 7c and 7d. At high scan rates, the deviation of the shape is related to the difference between the faster flowing electron velocity and the velocity of electrode reaction. So, there is a difficulty to form the electric double layer at the interface. A comparison of the current values for the synthesized GO and composites during the fourth cycle at a scan rate of 200 mV/s, is shown in Fig. 7e. The remarkable increase in current reflects an improvement in specific capacitance for the synthesized nano-composites and the optimum trend was recorded for S1. This behavior can be attributed to the higher density of charge carries and the well-known generation of SnO_2 nanoparticles due to the reduction of GO. Moreover, the bigger of the area under CV curve indicates an increment of specific capacitance which result from the increase of ions accessibility. SEM measurements confirm the large area of the synthesized sheets. Meanwhile, decoration of GO with nano particles diminish the space between GO layers and facility the ionic transition. We think that nanoparticles form a network for carrier transport.

Moreover, the specific capacitance was calculated from the well-known Eq. (1):

$$C_{sp} = \frac{\mathrm{d}q}{m.\mathrm{d}V} = \frac{\mathrm{d}q/\mathrm{d}t}{m.\mathrm{d}V/\mathrm{d}t} = \frac{I}{m.\mathrm{d}V/\mathrm{d}t}, \qquad (1)$$

where C_{sp} is specific capacitance of the electrodes, i is the current, dV/dt is the scan rate of the potential, and m is the mass of the active materials of the electrodes [31, 32].

Capacitance of GO, S1, and S2 is shown in Fig. 8.The capacitance of S1 is more than S2, due to the variation in surface morphology, dispersion of SnO_2 nano particles and the increase of current [33,34]. With increasing the scan rate, partiall stability in the capacitance values were observed.

4. CONCLUSION

Comparing with the conventional preparation method, the proposed new route does not require additional steps or heat treatment. Furthermore, it is cost ef-

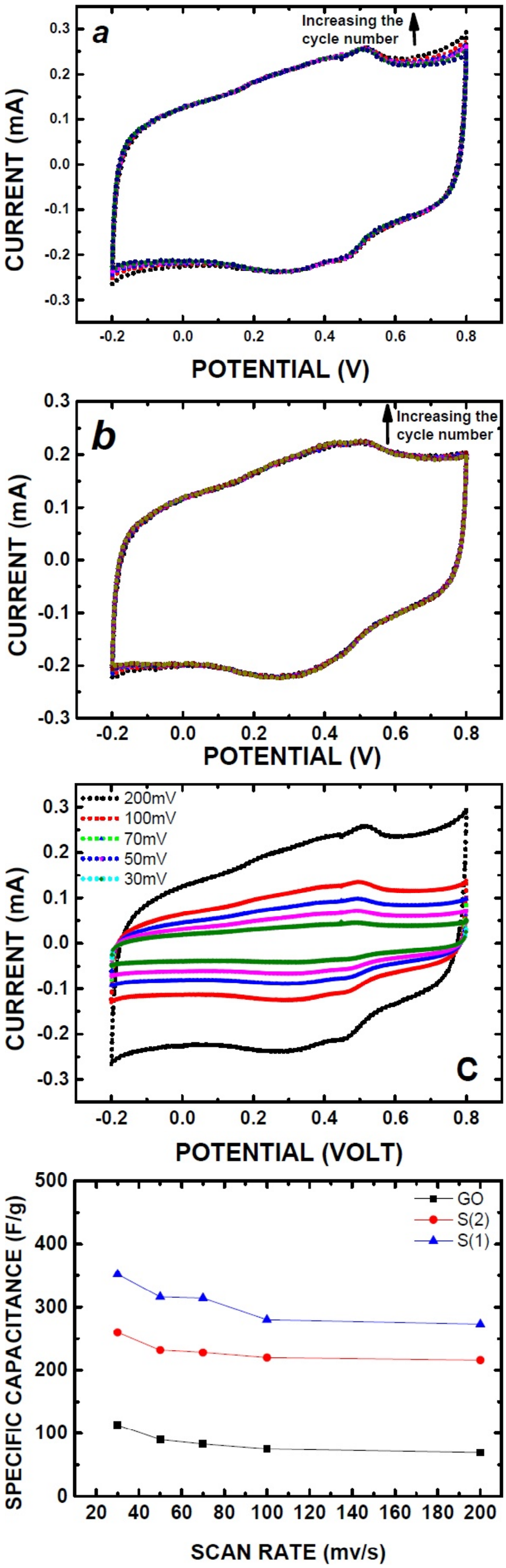

Fig. 8. The specific capacitance of GO, S1, and S2.

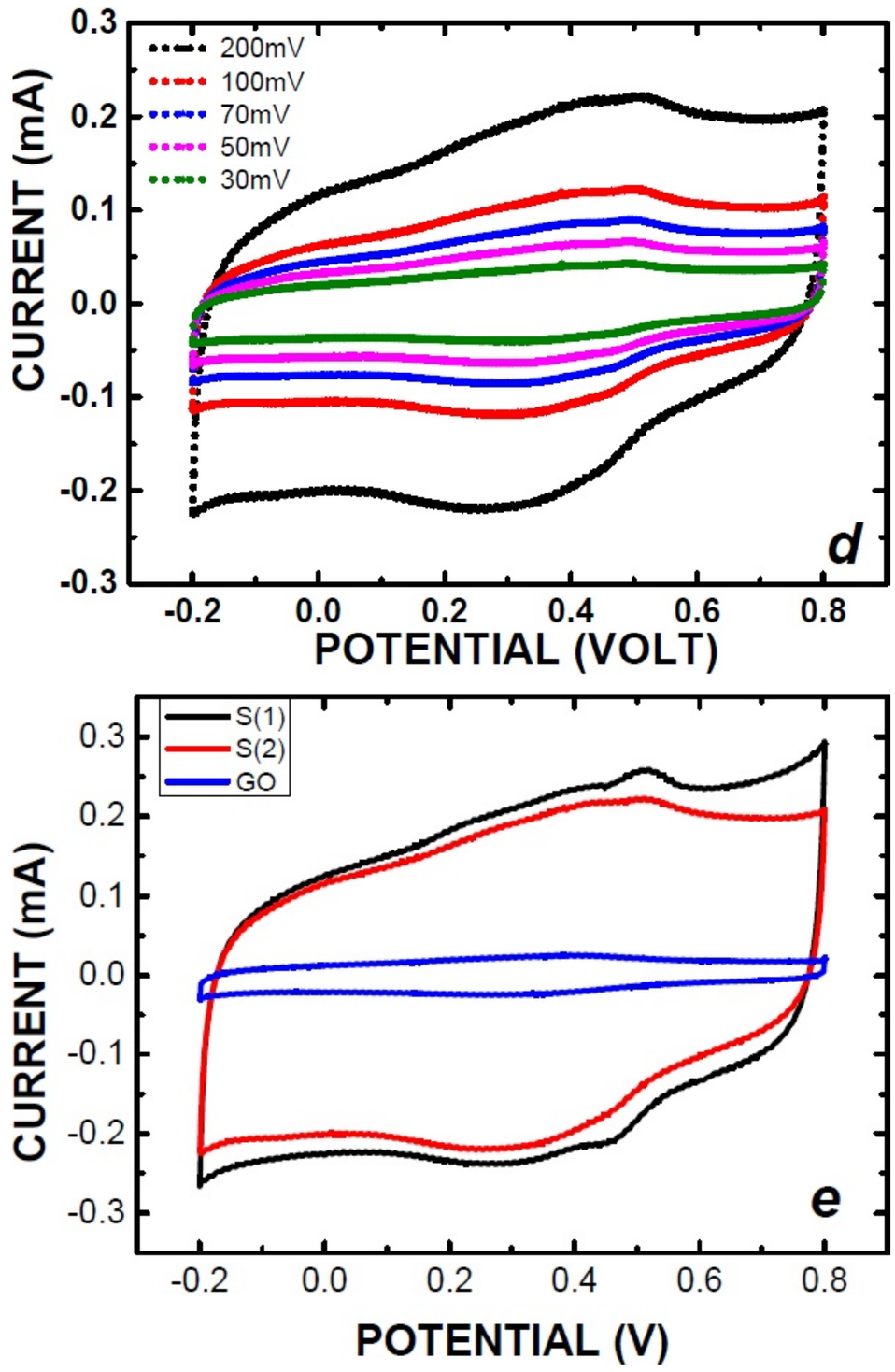

Fig. 7. CV at a scan rate of 200 mv/s for S1 (7a), S2 (7b) with different cycles, CV at different scan rates 30mv/s, 50mv/s, 70mv/s, 100mv/s and 200mv/s for S1 (7c), S2 (7d), and (7e) comparison of CV at scan rate of 200mv/s for GO, S1, and S2.

fective and applicable to different doping elements. The enhancement in the electrochemical performance is related to the following. First, SnO_2 can provide excellent electronic conducting channels. Second, the high surface area of GO enhances the capacitance. Third, GO accommodate the volumetric strain of SnO_2 nanoparticles.

REFERENCES

[1] Chenguang Liu, Zhenning Yu, David Neff, Aruna Zhamu and Bor Z. Jang // *Nano Lett.* **10** (2010) 4863.

[2] Tianju Fan, Wenjin Zeng, Qiaoli Niu, Songzhao Tong, Kaiyu Cai, Yidong Liu, Wei Huang, Yong

Min and Arthur J. Epstein // *Nanoscale Research Letters* **10 (1)** (2015) 1.
[3] Yan Wang, Zhiqiang Shi, Yi Huang, Yanfeng Ma, Chengyang Wang, Mingming Chen and Yongsheng Chen // *J. Phys. Chem. C* **113** (2009) 13103.
[4] M. Winter and J. O. Besenhard // *Electrochim. Acta* **45** (1999) 31.
[5] L.W. Ji, Z.K. Tan, T. Kuykendall, E.J. An, Y.B. Fu, V. Battaglia and Y.G. Zhang // *Energy Environ. Sci.* **4** (2011) 3611.
[6] K.S. Novoselov, A.K. Geim, S.V. Morozov, D. Jiang, Y. Zhang and S.V. Dubonos // *Science* **306** (2004) 666.
[7] A.K. Geim and k.S. Novoselov // *Nat. Mater.* **6** (2007) 183.
[8] S. Ding, D. Luan, F.Y.C. Boey, J.S. Chen and X.W. Lou // *Chem. Commun.* **47** (2011) 7155.
[9] S. Sladkevich, J. Gun, P.V. Prikhodchenko, V. Gutkin, A.A. Mikhaylov, V.M. Novotortsev, J.X. Zhu, D. Yang, H.H. Hng, Y.Y. Tay, Z. Tsakadze and O. Lev // *Nanotechnology* **23** (2012) 485601.
[10] C.K. Chan, H.L. Peng, G. Liu, K.M.L. Wrath, X.F. Zhang, R.A. Huggins and Y. Cui // *Nat. Nanotechnol.* **3** (2008) 31.
[11] Junfei Liang, Yue Zhao, Lin Guo and Lidong Li // *ACS Appl. Mater. Interfaces* **4** (2012) 5742.
[12] Y. Zhao, J.X. Li, Y.H. Ding and L.H. Guan // *RSC Adv.* **1** (2011) 852.
[13] B. Wang, D.W. Su, J. Park, H. Ahn and G.X. Wang // *Nanoscale Res. Lett.* **7** (2012) 215.
[14] M. Pumera // *Chem. Soc. Rev.* **39** (2010) 4146.
[15] E.J. Yoo, J. Kim, E. Hosono, H.S. Zhou, T. Kudo and I. Honma // *Nano Lett.* **8** (2008) 2277.
[16] G.X. Wang, X.P. Shen, J. Yao and J.S. Park // *Carbon* **47** (2009) 2049.
[17] William S. Hummers and Richard E. Offeman // *American chemical society* **80** (1958) 1339..
[18] A.N. Fouda, M.K. Abu Assy, Gaber El Enany and Nehad Yousf // *Fullerenes, Nanotubes and Carbon Nanostructures* **230** (2014) 618.
[19] Guoxiu Wang, Xiaoping Shen, Jane Yao and Jinsoo Park // *Carbon* **47/8** (2009) 2049.
[20] Jeffrey R. Potts, Daniel R. Dreyer, Christopher W. Bielawski and Rodney S. Ruoff // *Polymer* **52/1** (2011) 5.
[21] E-S M. Duraia, Z.A Mansurov and S.Zh. Tokmoldin // *Vacuum* **86** (2011) 232.
[22] A.N. Fouda, M.K. Abu-Assy and Nehad Yousf // *IOSR. J. App. Phy*. **6** (2014) 22.
[23] G.W. Beall, E-S M. Duraia, Q. Yu and Z. Liu // *Physica E* **56** (2014) 331.
[24] E-S M. Duraia, M. Burkitbaev, H. Mohamedbakr, Z. Mansurov and G.W. Beall // *Vacuum* **84** (2010) 464.
[25] El-Shazly M. Duraia, B. Henderson and Gary W. Beall // *Journal of Physics and Chemistry of Solids* **85** (2015) 86.
[26] Fenghua Li, Jiangfeng Song, Huafeng Yang, Shiyu Gan, Qixian Zhang, Dongxue Han, Ari Ivaska and Li Niu // *Nanotechnology* **20** (2009) 455602.
[27] Changdong Gu, Heng Zhang, Xiuli Wang and Jiangping Tu // *Materials Research Bulletin* **48** (2013) 4112.
[28] Xiangyang Zhou, Youlan Zou and Juan Yang // *Journal of Power Sources* **253** (2014) 287.
[29] Peichao Liana, Jingyi Wanga, Dandan Caib, Liangxin Dingb, Qingming Jiaa and Haihui Wang // *Electrochimica Acta* **116** (2014) 103.
[30] I. A. Courtney and J. R. Dahn // *Journal of the Electrochemical Society* **144** (1997) 2045.
[31] Z. Q. Li, C. J. Lu and Z. Luo // *Carbon* **45** (2007) 1686.
[32] J. Ye, H. Zhang and Q. Ran // *Power Sources* **212** (2012) 105.
[33] Bin Wang, Dahui Guan, Zan Gao, Jun Wang, Zhanshuang Li, Wanlu Yang and Lianhe Liu // *Materials Chemistry and Physics* **141** (2013) 1.
[34] Z. Qin, Z. Li, M. Zhang, B.C. Yang and R.A. Outlaw // *Journal of Power Sources* **217** (2012) 303.